

# Unexpected Influence of the Counteranion in the $\kappa^2$ vs $\kappa^3$ Hapticity of Polydentate *N*-Donor Ligands in $[\text{Rh}^{\text{I}}(\text{N-ligand})\text{L}_2]^+$ Complexes

Gabriel Aullón,<sup>†</sup> Glòria Esquiús, Agustí Lledós,\* Feliu Maseras, Josefina Pons, and Josep Ros\*

Departament de Química, Universitat Autònoma de Barcelona, 08193 Bellaterra, Barcelona, Spain

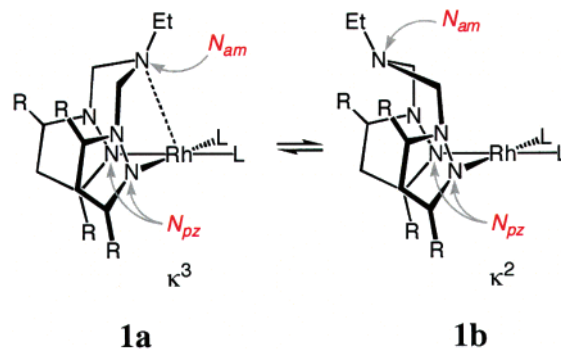
Received April 1, 2004

A study of the complexes  $[\text{Rh}(\text{N-ligand})\text{L}_2]^+$  in which *N*-ligand is bis(1-pyrazolylmethyl)ethylamine and L are cyclooctadiene or carbonyl ligands is presented. The presence of three nitrogen donor atoms opens the possibility that the *N*-ligand acts as a  $\kappa^2$  or a  $\kappa^3$  ligand. Experimental results show that it is coordinated in a  $\kappa^3$  coordination mode in the solid state, but both isomers coexist in solution. Theoretical calculations have been carried out to analyze the factors that determine the choice of the hapticity. The reproduction of the experimental stabilities requires the explicit consideration of the counteranion in the calculation. The transition state for the interconversion of  $\kappa^3$  and  $\kappa^2$  isomers has been located. The process takes place in one step, but involves simultaneous decoordination and inversion of the apical aminic nitrogen. A theoretical study of the hapticity of the related tris(pyrazolyl)borate complexes is also presented and compared with the results found in our system.

## Introduction

Although the four-coordinate square-planar geometry is the most common structure adopted by  $d^8$  transition metal complexes, five-coordinate square-pyramidal (or trigonal-bipyramidal) geometries are also possible.<sup>1</sup> This dichotomy between four and five coordination becomes apparent when multidentate ligands with several hapticity possibilities are coordinated to the metal. For instance, in the important family of compounds with general formula  $[\text{M}(\text{N-ligand})\text{L}_2]$  (*N*-polydentate ligand, L = monodentate ligand), when the *N*-ligand can act only as a bidentate ligand, a 16-electron complex with the expected square-planar geometry results. In contrast, the *N*-ligand with three nitrogen donor atoms can behave as a  $\kappa^2$  or  $\kappa^3$  ligand, leading to four-coordinate, formally 16-electron or five-coordinate (18-electron) species. Actually,  $[\text{Rh}(\text{N-ligand})\text{L}_2]$  compounds of rhodium(I) with three *N*-donor ligands are found in the solid state with  $\kappa^2$  or  $\kappa^3$  denticities. In solution an equilibrium can easily occur, due to a fast interconversion process between these geometries. A pioneering work of Oro et al. for tris(1-pyrazolylmethyl)amine complexes of rhodium(I) and iridium(I) showed from the infrared spectra in solution that these compounds are stereochemically nonrigid due to the presence of tetra- and pentacoordinate species resulting from the coordination of two or three pyrazolyl groups to the metal atom. Moreover, the <sup>1</sup>H NMR spectrum at room temperature suggests a rapid exchange on the NMR time scale.<sup>2</sup>

We have recently proved the flexibility of the bis((3,5-dimethyl-1-pyrazolyl)methyl)ethylamine ( $\text{N}_3^{\text{Me}}$ ) ligand, which adapts its bonding mode ( $\kappa^2$  or  $\kappa^3$ ) to various electronic and steric situations around the rhodium(I) atom.<sup>3</sup> The complexes  $[\text{Rh}(\text{N}_3^{\text{Me}})\text{L}_2]^+$ , in which  $\text{N}_3^{\text{Me}}$  is the tripodal pyrazole-amine-pyrazole ligand and  $\text{L}_2$  is 1,5-cyclooctadiene (cod) or two carbonyl molecules, were analytically, spectroscopically (IR and <sup>1</sup>H and <sup>13</sup>C{<sup>1</sup>H} NMR), and structurally (X-ray diffraction) characterized. The molecular structure shows that the  $\text{N}_3^{\text{Me}}$  ligand is coordinated in a  $\kappa^3$  mode of bonding (1a)



with a geometry around the rhodium atom defined as square-pyramidal. The pyrazole rings and the  $\text{L}_2$  ligands determine the basal plane, and the apical position is occupied by the aminic nitrogen.<sup>3</sup> Similar rhodium and iridium complexes with analogous ligands have been prepared by Gal et al.,<sup>4–8</sup> including complexes with nonsymmetric *N*-ligands of pyrazole-amine-pyridine<sup>4,5</sup>

<sup>†</sup> Present address: Departament de Química Inorgànica and Centre de Recerca en Química Teòrica, Universitat de Barcelona, Diagonal 647, 08028 Barcelona, Spain.

(1) (a) Kepert, D. L. *Inorganic Stereochemistry*; Springer-Verlag: Berlin, 1982; Vol. 6. (b) Holmes, R. R. *Prog. Inorg. Chem.* **1984**, *32*, 119. (c) Auf der Heyde, T. *Angew. Chem., Int. Ed. Engl.* **1994**, *33*, 823.

(2) Fernández, M. J.; Rodríguez, M. J.; Oro, L. A. *Polyhedron* **1991**, *10*, 1595.

(3) Mathieu, R.; Esquiús, G.; Lugan, N.; Pons, J.; Ros, J. *Eur. J. Inorg. Chem.* **2001**, 2683.

and pyrrole-amine-pyridine types.<sup>5,7</sup> The preference of the strongest  $\sigma$ -donor ligands for the basal position can be rationalized with molecular orbital arguments.<sup>9</sup>

Although in the solid state only the  $\kappa^3$  isomer is observed, the NMR spectra show the existence of two isomers (**1a** and **1b**) in solution. In several cases variable-temperature NMR studies give evidence of a  $\kappa^3 \leftrightarrow \kappa^2 \leftrightarrow \kappa^3$  interconversion, through a mechanism with initial decoordination of  $\text{N}_{am}$ , followed by the inversion of configuration at this nitrogen atom and subsequent coordination of  $\text{N}_{am}$  on the other face of the plane.<sup>4–6</sup> In this field, an extensive bibliography can be found for the polydentate  $N$ -ligands related with poly(pyrazolyl)-borates known as scorpionates,<sup>10,11</sup> which constitute a system of reference for our study.

In the quest for the factors determining the hapticity ( $\kappa^2$  vs  $\kappa^3$ ) of the  $\text{N}_3^R$  ligands we have synthesized new complexes in this family and performed a theoretical study on the structure, relative energies, and fluxional behavior of the isomers of  $[\text{Rh}(\text{N}_3^R)\text{L}_2]^+$  complexes. We report here the synthesis and characterization of two new complexes containing the bis(1-pyrazolylmethyl)-ethylamine ( $\text{N}_3^H$ ) ligand,<sup>12</sup> which also present an equilibrium in solution between the  $\kappa^2$  and  $\kappa^3$  modes of bonding. Comparison of the behavior of  $\text{N}_3^{\text{Me}}$  and  $\text{N}_3^H$  ligands will allow us to weigh the steric influence of the pyrazol substituents in the equilibrium. In addition we present a density functional (DFT) study of the entire family of  $[\text{Rh}(\text{N}_3^R)\text{L}_2]^+$  compounds in an attempt to understand the molecular geometries and their fluxional behavior. The effect of the presence of the counteranions in the crystal will also be analyzed computationally through DFT calculations. To broaden the scope of our study, we have considered not only complexes having our  $\text{N}_3^R$  ligands but also complexes with the well-known family of hydridotris(1-pyrazolyl)borate  $\text{HB}\{\text{pz}^R\}_3$  and related ligands, which we have abbreviated as  $\text{Tp}^R$ . This comparison will illustrate the specificity of our  $\text{N}_3^R$  ligands among other tridentate  $N$ -ligands.

## Results and Discussion

**Synthesis of  $[\text{Rh}(\text{N}_3^H)\text{L}_2]^+$  Complexes.** In the same way as the reported  $\text{N}_3^{\text{Me}}$ ,<sup>3</sup> the  $\text{N}_3^H$  ligand reacts with  $[\text{Rh}(\text{cod})(\text{thf})_2][\text{BF}_4]$  (generated in situ from the reaction of  $[\text{Rh}_2\text{Cl}_2(\text{cod})_2]$  and  $\text{AgBF}_4$  in thf) to give the complex  $[\text{Rh}(\text{N}_3^H)(\text{cod})][\text{BF}_4]$  in 87% yield. The proton NMR

(4) de Bruin, B.; Brands, J. A.; Donners, J. J. M.; Donners, M. P. J.; de Gelder, R.; Smits, J. M. M.; Gal, A. W.; Spek, A. L. *Chem. Eur. J.* **1999**, *5*, 2921.

(5) de Bruin, B.; Kicken, R. J. N. A. M.; Suos, N. A. F.; Donners, M. P. J.; den Reijer, C. J.; Sandee, A. J.; de Gelder, R.; Smits, J. M. M.; Gal, A. W.; Spek, A. L. *Eur. J. Inorg. Chem.* **1999**, 1581.

(6) Sciarone, T.; Hoogboom, J.; Schlebos, P. P. J.; Budzelaar, P. H. M.; de Gelder, R.; Smits, J. M. M.; Gal, A. W. *Eur. J. Inorg. Chem.* **2002**, 457.

(7) de Bruin, B.; Peters, T. P. J.; Sous, N. N. F. A.; de Gelder, R.; Smits, J. M. M.; Gal, A. W. *Inorg. Chim. Acta* **2002**, *337*, 154.

(8) de Bruin, B.; Peters, T. P. J.; Wilting, J. B. M.; Thewissen, S.; Smits, J. M. M.; Gal, A. W. *Eur. J. Inorg. Chem.* **2002**, 2671.

(9) Rossi, A. R.; Hoffmann, R. *Inorg. Chem.* **1975**, *14*, 365.

(10) (a) Trofimenko, S. *Chem. Rev.* **1993**, *93*, 943. (b) Trofimenko, S. *Scorpionates: The Coordination Chemistry of Polypyrazolylborate Ligands*; Imperial College Press: London, 1999. (c) Jalón, F. A.; Manzano, B. R.; Gómez de la Torre, F.; Guerrero, A. M.; Rodríguez, A. M., Eds. *Dynamic Processes in Palladium and Platinum Complexes Coordinated on Scorpionate and Pyrazolylazine Type Ligands*; Società Chimica Italiana: Roma, 1999; Vol. 3.

(11) Kitajima, N.; Tolman, W. B. *Prog. Inorg. Chem.* **1995**, *43*, 418.

(12) Driessen, W. L. *Recl. Trav. Chim. Pays-Bas* **1982**, *101*, 441.

**Table 1. Experimental Data on the  $\kappa^2:\kappa^3$  Equilibrium Ratio in Solution for the  $[\text{Rh}(\text{N}_3^R)\text{L}_2]^+$  (L = cod/2, CO; R = H, Me) Complexes**

compound R	L		reference
	cod/2	CO	
H	2:1	1:1.2	this work
Me	2:1	1:10	ref 3

spectrum of the complex shows the presence of two isomers in a 2:1 ratio. The  $^1\text{H}$  NMR ethyl group signals of the minor isomer are more deshielded than those of the major one, suggesting that the nitrogen of the amine group in the minor isomer is bonded to rhodium in a  $\kappa^3$  mode of bonding.

Bubbling carbon monoxide into a solution of  $[\text{Rh}(\text{N}_3^H)(\text{cod})][\text{BF}_4]$  in dichloromethane at room temperature, the 1,5-cyclooctadiene ligand was replaced by two molecules of CO, giving the  $[\text{Rh}(\text{N}_3^H)(\text{CO})_2][\text{BF}_4]$  complex, which can be isolated as a yellow solid in 78% yield. The infrared spectrum in the  $\nu_{\text{CO}}$  region shows four strong absorption bands at 2088 and 2021  $\text{cm}^{-1}$  and two medium at 2109 and 2049  $\text{cm}^{-1}$ , which agree with the presence of two isomers. The  $^1\text{H}$  NMR spectrum also corroborated the presence of these isomers in the ratio 1:1.2, in this case the complex with a  $\kappa^3$ -coordinated  $\text{N}_3^H$  ligand being the major isomer.

The experimental data on the  $\kappa^2:\kappa^3$  equilibrium ratio in solution for the entire series of  $[\text{Rh}(\text{N}_3^R)\text{L}_2]^+$  (L = cod/2, CO; R = H, Me) (Table 1) led us to conclude that the square-pyramidal  $\kappa^3$  structures are strongly favored by the presence of carbonyl ligands and, to a lesser extent, by the methyl substituents in the  $N$ -ligand. In the solution equilibrium, the higher amount of the  $\kappa^3$  isomer (1:10) is found for  $[\text{Rh}(\text{N}_3^{\text{Me}})(\text{CO})_2]^+$ .

**Optimized Molecular Structures.** Density functional calculations were performed on complexes of formula  $[\text{Rh}(\text{N}_3^R)\text{L}_2]^+$  (L = cod/2, CO; R = H, Me), considering in each case the two possible isomers corresponding to the different coordination of the  $\text{N}_3^R$  ligand:  $\kappa^3$  (**1a**) and  $\kappa^2$  (**1b**). The main parameters of the optimized structures are presented in Table 2, and their coordinates are available as Supporting Information.

The two optimized geometries of  $[\text{Rh}(\text{N}_3^R)\text{L}_2]^+$  can be clearly assigned to  $\kappa^3$  and  $\kappa^2$  coordination modes of the  $N$ -ligand. As an example, the structures of both isomers of  $[\text{Rh}(\text{N}_3^{\text{Me}})(\text{CO})_2]^+$  are shown in Figure 1. Similar geometries are obtained for related complex having the cod and the  $\text{N}_3^H$  ligands. The  $\kappa^2$  isomers present a perfectly planar sphere of coordination for rhodium(I) atoms ( $\Sigma\text{Rh} = 360.0^\circ$ ), as can be expected for a square-planar  $d^8\text{-ML}_4$  transition metal complex, and the  $\text{N}_{am}$  atom is far from the metal ( $\text{Rh}-\text{N}_{am} > 3.8 \text{ \AA}$ ). The rhodium atom lies on the plane defined by the four ligands, showing deviations of only 0.02  $\text{Å}$  ( $\text{L}_2 = \text{cod}$ ) and 0.01  $\text{Å}$  ( $\text{L} = \text{CO}$ ). On the contrary,  $\kappa^3$  forms show  $\text{Rh}-\text{N}_{am}$  distances between 2.74 and 2.87  $\text{Å}$ , considerably shorter than the sum of van der Waals radii ( $\sim 3.4 \text{ \AA}$ ),<sup>9</sup> and a slight pyramidalization of the Rh atom, which lies 0.13  $\text{Å}$  ( $\text{L}_2 = \text{cod}$ ) and 0.10  $\text{Å}$  ( $\text{L} = \text{CO}$ ) above the plane defined by the four basal ligands. Both geometrical features agree with the existence of a  $\text{Rh}-\text{N}_{am}$  interaction.<sup>13</sup> For the ligands on the basal plane the  $\text{Rh}-\text{N}_{pz}$  distances are longer in the  $\kappa^2$  isomer than in

(13) Aullón, G.; Alvarez, S. *Inorg. Chem.* **1996**, *35*, 3137.

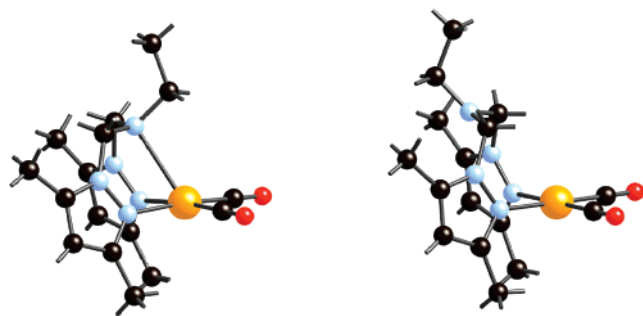
**Table 2.** Optimized Geometrical Parameters for the  $\kappa^2$  and  $\kappa^3$  Isomers of Complexes  $[\text{Rh}(\text{N}_3^R)\text{L}_2]^+$  ( $\text{L} = \text{cod}/2, \text{CO}$ ;  $\text{R} = \text{H}, \text{Me}$ ) and  $[\text{Rh}(\text{N}_3^R)(\text{CO})]^+$  ( $\text{R} = \text{H}, \text{Me}$ )<sup>a</sup>

parameter <sup>b</sup>	$[\text{Rh}(\text{N}_3^H)(\text{cod})]^+$		$[\text{Rh}(\text{N}_3^H)(\text{CO})_2]^+$		$[\text{Rh}(\text{N}_3^H)(\text{CO})]^+$
	$\kappa^3$	$\kappa^2$	$\kappa^3$	$\kappa^2$	$\kappa^3$
Rh–L	2.048	2.068	1.887	1.898	1.866
L–L'	1.403	1.397	1.145	1.143	1.149
Rh–N <sub>pz</sub>	2.172	2.152	2.137	2.127	2.051
Rh–N <sub>am</sub>	2.870	3.850	2.844	3.832	2.181
L–Rh–L	87.0	87.0	91.2	91.9	
N <sub>pz</sub> –Rh–N <sub>pz</sub>	84.4	87.7	85.7	88.0	161.5
N <sub>pz</sub> –Rh–L	93.9	92.6	91.3	90.0	99.2
N <sub>am</sub> –Rh–N <sub>pz</sub>	68.1		68.8		80.8
N <sub>am</sub> –Rh–L	117.6		115.3		178.0
$\Sigma \text{Rh}^c$	359.2	360.0	359.4	360.0	360.0
$\Sigma \text{N}_{am}^c$	345.8	358.3	346.0	358.6	338.4

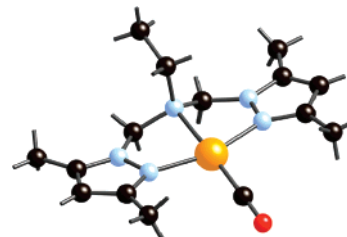
parameter <sup>b</sup>	$[\text{Rh}(\text{N}_3^{\text{Me}})(\text{cod})]^+$		$[\text{Rh}(\text{N}_3^{\text{Me}})(\text{CO})_2]^+$		$[\text{Rh}(\text{N}_3^{\text{Me}})(\text{CO})]^+$
	$\kappa^3$	$\kappa^2$	$\kappa^3$	$\kappa^2$	$\kappa^3$
Rh–L	2.048 (1.985)	2.069	1.884 (1.801)	1.895	1.859 (1.809)
L–L'	1.404 (1.401)	1.397	1.146 (1.147)	1.144	1.151 (1.146)
Rh–N <sub>pz</sub>	2.187 (2.165)	2.168	2.144 (2.094)	2.135	2.058 (2.018)
Rh–N <sub>am</sub>	2.741 (2.514)	3.802	2.766 (2.565)	3.775	2.179 (2.120)
L–Rh–L	86.8 (87.5)	86.9	91.3 (90.1)	92.2	
N <sub>pz</sub> –Rh–N <sub>pz</sub>	82.5 (82.0)	86.4	86.0 (90.4)	89.9	161.1 (161.8)
N <sub>pz</sub> –Rh–L	94.9 (94.4)	93.4	91.1 (89.1)	88.1	99.4 (99.1)
N <sub>am</sub> –Rh–N <sub>pz</sub>	70.5 (73.8)		70.3 (72.0)		80.6 (80.9)
N <sub>am</sub> –Rh–L	115.2 (116.0)		113.7 (115.9)		176.0 (179.3)
$\Sigma \text{Rh}^c$	359.1 (358.2)	360.0	359.5 (358.7)	360.0	360.0 (360.0)
$\Sigma \text{N}_{am}^c$	341.4 (336.8)	350.8	343.8 (334.8)	353.5	338.4 (338.1)

<sup>a</sup> Distances are in Å, angles in deg, mean experimental values in parentheses.<sup>3</sup> <sup>b</sup> L–L' are the C–O and C=C distances in carbonyl and diene ligands, respectively. For N<sub>pz</sub> or N<sub>am</sub> see 1. <sup>c</sup>  $\Sigma \text{Atom}$  is the sum of all the bond angles around this atom.

**Figure 1.** Optimized molecular structures of the  $\kappa^3$  (left) and  $\kappa^2$  (right) isomers of  $[\text{Rh}(\text{N}_3^{\text{Me}})(\text{CO})_2]^+$ .

the  $\kappa^3$  ones, with the largest difference found for cyclooctadiene complexes. Steric requirements also play a role in the molecular conformation of the complex,<sup>5</sup> as shown by the increase of about 4° in the N<sub>pz</sub>–Rh–N<sub>pz</sub> angle in  $\kappa^2$  isomers with respect to the  $\kappa^3$  ones, imposed by the position of the aliphatic chain of the N-ligand between the two pyrazolyl rings. An increase of the Rh–L distances are observed for L ligands in  $\kappa^2$  isomers, with a concomitant decrease of C=C (diolefin) or C≡O (carbonyl) distances, in agreement with the infrared spectroscopy data.<sup>3</sup>

The influence of the nature of L in the coordination of the N-ligand can be inferred by comparing the structures of  $[\text{Rh}(\text{N}_3^R)(\text{cod})]^+$  and  $[\text{Rh}(\text{N}_3^R)(\text{CO})_2]^+$ . As already found in the X-ray structures, the Rh–N distances are slightly shorter (~0.03 Å) for carbonyl complexes. More important is the decrease of the L–Rh–L angle from 92° (L = CO) to 87° (L = cod) due to the chelating nature of the cyclooctadiene ligand, although without affecting the sum of angles around the rhodium atom. To analyze the influence of the coordination in the N-ligand, we have also calculated

**Figure 2.** Optimized geometry of  $[\text{Rh}(\text{N}_3^{\text{Me}})(\text{CO})]^+$ , a tetracoordinated rhodium(I) complex with  $\kappa^3$  coordination of the N-ligand.

the square-planar compounds  $[\text{Rh}(\text{N}_3^R)(\text{CO})]^+$  (R = H, Me) with  $\kappa^3$  coordination of the N-ligand (Figure 2). The calculated Rh–N<sub>pz</sub> distances (2.06 Å) are remarkably shorter than the Rh–N<sub>am</sub> ones (2.18 Å), reproducing the experimental trend found in the X-ray structure of  $[\text{Rh}(\text{N}_3^{\text{Me}})(\text{CO})]^+$ .<sup>3</sup> As previously observed in other complexes having d<sup>8</sup> transition metals such as palladium(II)<sup>14</sup> and gold(III),<sup>15</sup> this effect can be attributed to the *trans* influence of the carbonyl ligand more than to the different hybridization of the N<sub>pz</sub> and N<sub>am</sub> nitrogen atoms.<sup>4,5</sup>

When H groups are replaced by Me ones in positions 3 and 5 of the pyrazolyl rings, no changes are found for the L ligands, although a lengthening of 0.01 Å for the Rh–N<sub>pz</sub> and a shortening of 0.1 Å for the Rh–N<sub>am</sub> bond in the  $\kappa^3$  isomer can be observed. The aminic nitrogen atom is more pyramidalized in N<sub>3<sup>Me</sup></sub> complexes than in related N<sub>3<sup>H</sup></sub> ones. All these changes are consistent with a stronger apical bond for the N<sub>3<sup>Me</sup></sub> ligand. Despite the variations introduced by the presence of methyl groups,

(14) Meneghetti, S. P.; Lutz, P. J.; Kress, J. *Organometallics* **2001**, *20*, 5050.

(15) Nardin, G.; Randaccio, L.; Annibale, G.; Natile, G.; Pitteri, B. *J. Chem. Soc., Dalton Trans.* **1980**, 220.

**Table 3. Relative Energies (in  $\text{kJ}\cdot\text{mol}^{-1}$ ) of the  $\kappa^2$  and  $\kappa^3$  Isomers of  $[\text{Rh}(\text{N}_3^{\text{R}})\text{L}_2]^+$  Compounds (L = cod/2 or CO; R = H, Me)<sup>a</sup>**

compound		isomer	
R	L	$\kappa^3$	$\kappa^2$
H	cod/2	0.0	-31.3 (-45.7)
Me	cod/2	0.0	-25.4 (-40.5)
H	CO	0.0	-22.9 (-44.2)
Me	CO	0.0	-15.7 (-36.7)

<sup>a</sup> In parentheses, relative energy of the free ligands, calculated at the geometry that they adopt in the  $\kappa^2$  and  $\kappa^3$  isomers of each complex.

the calculated Rh– $\text{N}_{\text{am}}$  apical bond lengths are considerably longer than the experimental ones<sup>3</sup> (2.74 vs 2.51 Å and 2.77 vs 2.56 Å for cyclooctadiene and carbonyl complexes, respectively). However, the long experimental distances are consistent with a weak Rh– $\text{N}_{\text{am}}$  interaction, and it could be expected that large variations in this distance have only minor consequences on the energy of the complex. To assess the validity of this hypothesis, we fixed the Rh– $\text{N}_{\text{am}}$  distances at their experimental values and optimized the rest of the geometrical parameters. A destabilization of only 4.8  $\text{kJ}\cdot\text{mol}^{-1}$  with respect to the minimum structures was found, indicating that packing crystal forces can be responsible for the discrepancy.

**Relative Stabilities of  $\kappa^2$  and  $\kappa^3$  Isomers.** The relative energies of the  $\kappa^2$  and  $\kappa^3$  isomers are given in Table 3. As summarized in the Introduction, the experimental data indicate that in the solid state the  $\kappa^3$  coordination mode is favored, whereas similar energies can be inferred for the  $\kappa^2$  and  $\kappa^3$  isomers from the coexistence in solution of both isomers of complexes  $[\text{Rh}(\text{N}_3^{\text{R}})(\text{cod})]^+$  and  $[\text{Rh}(\text{N}_3^{\text{R}})(\text{CO})_2]^+$ .

The results of our energy calculations do not agree with these experimental data. The  $\kappa^2$  structures are always found more stable than the  $\kappa^3$  ones for the series of  $[\text{Rh}(\text{N}_3^{\text{R}})\text{L}_2]^+$  (L = cod/2 or CO; R = H, Me) complexes considered, in contrast with the experimental results. To assess the role that entropic effect plays in the relative stability of the  $\kappa^2$  and  $\kappa^3$  isomers,  $\Delta G$  values have been calculated for  $[\text{Rh}(\text{N}_3^{\text{Me}})\text{L}_2]^+$  (L = cod/2 or CO). From the  $\Delta G$  values the  $\kappa^2$  isomer is still preferred (-30.5 and -17.2  $\text{kJ}\cdot\text{mol}^{-1}$  for L = cod/2 and CO, respectively), with minor changes from the  $\Delta E$  values (-25.4 and -15.7  $\text{kJ}\cdot\text{mol}^{-1}$  for L = cod/2 and CO, respectively). Despite the different degrees of freedom of the  $\kappa^2$  and  $\kappa^3$  isomers, entropic effects have little influence on their relative stabilities.

Although the preference for the  $\kappa^3$  coordination mode is not properly reproduced, the stability trends can be related with the experimental behavior. When methyl groups in the pyrazolyl ring are substituted by hydrogen atoms, the stability of the  $\kappa^2$  isomer compared with the  $\kappa^3$  isomer increases about 6–7  $\text{kJ}\cdot\text{mol}^{-1}$ . Similarly, complexes having cyclooctadiene as a ligand,  $[\text{Rh}(\text{N}_3^{\text{R}})(\text{cod})]^+$ , present more stability of the  $\kappa^2$  structures than the carbonyl ones by about 9  $\text{kJ}\cdot\text{mol}^{-1}$ . From the calculations the most favorable system for  $\kappa^3$  hapticity of the  $\text{N}$ -donor ligand is that with L = CO and R = Me, in agreement with that found experimentally (see Table 1). The reduced basicity of the  $\text{Rh}^{\text{I}}$  center caused by the presence of the  $\pi$ -acceptor carbonyl ligands can account for the preference for pentacoordination in  $[\text{Rh}(\text{N}_3^{\text{R}})-$

$(\text{CO})_2]^+$ . The value of the L–M–L angle has also been pointed out as a factor at work stabilizing preferentially one coordination mode. Recently, Espinet et al. have found in rhodium(I) complexes with a related three  $\text{N}$ -donor ligand that dienes with small angle L–M–L favor the  $\kappa^3$  coordination mode.<sup>16</sup>

The change in coordination mode implies not only coordination/decoordination of the aminic nitrogen from the metal but an important reorganization of the aminic part of the ligand. To analyze if there is an intrinsic preference of the ligand for a coordination mode, we have calculated the energy of the free  $\text{N}_3^{\text{R}}$  ligands, at the geometry that is adopted in both the  $\kappa^2$  and the  $\kappa^3$  isomers of each complex (Table 3, values in parentheses). Comparing the energy difference between the two forms of the free ligands, we can conclude that the  $\text{N}$ -ligand always prefers the conformation adopted in the  $\kappa^2$  coordination mode. The interaction of the  $\text{N}_3^{\text{R}}$  ligand with the  $\text{RhL}_2$  fragment decreases this preference by 15 and 21  $\text{kJ}\cdot\text{mol}^{-1}$  for the  $\{\text{Rh}(\text{cod})\}$  and  $\{\text{Rh}(\text{CO})_2\}$  units, respectively, with almost no influence of the R substituent.

**Effect of the Counteranion.** The inability of our calculations to correctly reproduce the relative stabilities of the  $\kappa^2$  and  $\kappa^3$  isomers when our  $\text{N}_3^{\text{R}}$  ligands are present contrasts with the good agreement with the experimental values we have obtained for the relative energies of the  $\kappa^2$  and  $\kappa^3$  isomers of  $[\text{Rh}(\text{Tp}^{\text{R}})(\text{CO})_2]$  complexes (see later on). However, there is a big difference between the  $\text{N}_3^{\text{R}}$  and  $\text{Tp}^{\text{R}}$  complexes, related to the charge of the  $\text{N}$ -donor ligand: whereas the  $\text{Rh}^{\text{I}}$  complexes with the tris(1-pyrazolyl)borate ligands are neutral, those with the bis(1-pyrazolylmethyl)ethylamine ligands are cationic, and a counteranion is always present. There is an increasing amount of data proving that counterions are not only spectators in organometallic chemistry and that ion-pairing can influence organometallic structures and reaction mechanisms.<sup>17</sup> The  $\kappa^3$  isomer of  $[\text{Rh}(\text{N}_3^{\text{Me}})(\text{cod})]^+$  was obtained with  $[\text{BF}_4]^-$  as a counteranion and was structurally characterized by X-ray crystallography.<sup>3</sup> The complex crystallizes with three independent ion pairs per unit cell, in such a way that each cation has three  $[\text{BF}_4]^-$  anions at  $\text{Rh}\cdots\text{B}$  distances between 6 and 8 Å: one is found with a  $\text{Rh}\cdots\text{B}$  distance of 7.427 Å on the aminic arm side, looking at the  $\text{CH}_2$  groups that link the  $\text{N}_{\text{am}}$  and the pyrazolyl rings (region A); the second one is placed 6.066 Å above the metal, in a direction perpendicular to the basal plane (region B); and the third one lies on the pyrazolyl side, between the two rings with a  $\text{Rh}\cdots\text{B}$  distance of 7.869 Å (region C). We have introduced the counteranion in the calculations, placing a  $[\text{BF}_4]^-$  in the three regions and optimizing independently each ion

(16) Casares, J. A.; Espinet, P.; Martín-Alvarez, J. M.; Espino, G.; Pérez-Manrique, M.; Vattier, F. *Eur. J. Inorg. Chem.* **2001**, 289.

(17) (a) Macchioni, A.; Zuccaccia, C.; Clot, E.; Gruet, K.; Crabtree, R. H. *Organometallics* **2001**, *20*, 2367. (b) Malefetse, T.; Swiegers, G. F.; Coville, N. J.; Fernandes, M. A. *Organometallics* **2002**, *21*, 2898. (c) Kovacevic, A.; Gründemann, S.; Miecznikowski, J. R.; Clot, E.; Eisenstein, O.; Crabtree, R. H. *Chem. Commun.* **2002**, 2580. (d) Gruet, K.; Clot, E.; Eisenstein, O.; Lee, D. H.; Patel, B.; Macchioni, A.; Crabtree, R. H. *New J. Chem.* **2003**, *27*, 80. (e) Miecznikowski, J. R.; Gründemann, S.; Albrecht, M.; Mégret, C.; Clot, E.; Faller, J. W.; Eisenstein, O.; Crabtree, R. H. *Dalton Trans.* **2003**, 831. (f) Anil Kumar, P. G.; Pregonis, P. S.; Goicochea, J. M.; Whittlesey, M. K. *Organometallics* **2003**, *22*, 2956. (g) Basallote, M. G.; Besora, M.; Durán, J.; Fernández-Trujillo, M. J.; Lledós, A.; Máñez, M. A.; Maseras, F. J. *Am. Chem. Soc.* **2004**, *126*, 2320.

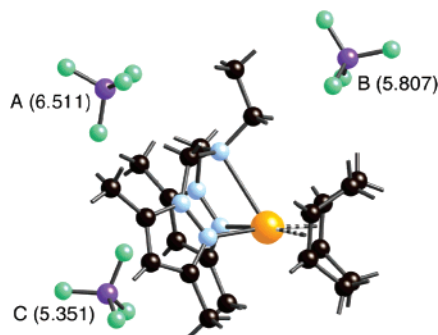


**Figure 3.** Position of the  $[\text{BF}_4]^-$  counteranion in the optimized structures of the  $[\text{Rh}(\kappa^3\text{-N}_3^{\text{Me}})(\text{cod})]^+\cdots[\text{BF}_4]^-$  ion pairs. In parentheses the optimized  $\text{Rh}\cdots\text{B}$  distances (Å) are shown.

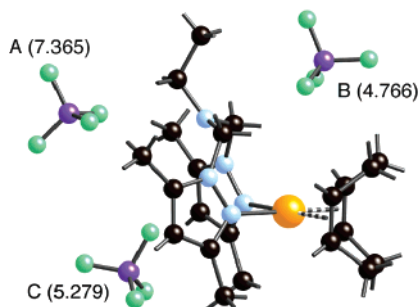


**Figure 4.** Position of the  $[\text{BF}_4]^-$  counteranion in the optimized structures of the  $[\text{Rh}(\kappa^2\text{-N}_3^{\text{Me}})(\text{cod})]^+\cdots[\text{BF}_4]^-$  ion pairs. In parentheses the optimized  $\text{Rh}\cdots\text{B}$  distances (Å) are shown.

pair, for both the  $\kappa^2$  and  $\kappa^3$  isomers of  $[\text{Rh}(\text{N}_3^{\text{Me}})(\text{cod})]^+$ . In agreement with the X-ray data, three ion-pair minima have been found, with the  $[\text{BF}_4]^-$  in the three regions. The placement of the anion in the optimized structures is shown in Figure 3 ( $\kappa^3$  isomer) and Figure 4 ( $\kappa^2$  isomer).

The  $\text{Rh}\cdots\text{B}$  distance for the anion in region C is not affected by the change in the coordination mode of the  $\text{N}_3^{\text{Me}}$  ligand. However the position of the anions in regions A and B is notably modified by changing the hapticity of the ligand. Going from  $\kappa^2$  to  $\kappa^3$  the aminic arm is pivoting, approaching the metal. As a consequence, the  $[\text{BF}_4]^-$  in region A also approaches the metal, and the  $\text{Rh}\cdots\text{B}$  distance decreases by 0.8 Å. The opposite happens for the  $[\text{BF}_4]^-$  in region B (the  $\text{Rh}\cdots\text{B}$  distance increases 1 Å). Because the  $[\text{Rh}(\text{N}_3^{\text{Me}})(\text{cod})]^+\cdots[\text{BF}_4]^-$  interaction is mainly ionic in character, we can expect it will be very dependent on the  $\text{Rh}\cdots\text{B}$  distance. Indeed this is the case. The calculated absolute values for this interaction are not meaningful, because they correspond to a gas phase interaction between two charged species, but the energy difference between the  $\kappa^2$  and  $\kappa^3$  isomers of the  $[\text{Rh}(\text{N}_3^{\text{Me}})(\text{cod})]^+\cdots[\text{BF}_4]^-$  ion pairs will indicate how the counteranion is affecting their relative stabilities. The results are summarized in Figure 5.

The energy differences between both isomers due to the different anion-cation interactions are in the same range as the  $\kappa^2$  vs  $\kappa^3$  energy difference found in the cation. Without counteranion, the  $\kappa^2$  structure is more stable than the  $\kappa^3$ , with a  $E(\kappa^2) - E(\kappa^3)$  energy difference of  $-25.4 \text{ kJ}\cdot\text{mol}^{-1}$ . When the counteranion is placed in the A region, this energy difference changes to  $+36.9$

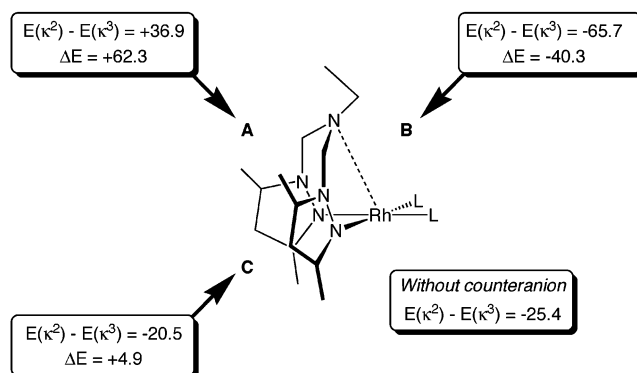


**Figure 5.** Schematic representation of the relative stabilities of the  $\kappa^2$  and  $\kappa^3$  isomers of  $[\text{Rh}(\text{N}_3^{\text{Me}})(\text{cod})]^+$  depending on the position of the  $[\text{BF}_4]^-$  counteranion.  $\Delta E$  is defined as the difference of  $E(\kappa^2) - E(\kappa^3)$  with and without counteranion. A positive value means preferential stabilization of the  $\kappa^3$  form. Energies are in  $\text{kJ}\cdot\text{mol}^{-1}$ .

$\text{kJ}\cdot\text{mol}^{-1}$ , reversing the stability ordering. Thus, the counteranion in region A stabilizes notably ( $62.3 \text{ kJ}\cdot\text{mol}^{-1}$ ) the  $\kappa^3$  isomer.  $[\text{BF}_4]^-$  in the B region increases to  $-65.7 \text{ kJ}\cdot\text{mol}^{-1}$  the relative stability of the  $\kappa^2$  isomer, whereas that in the C region slightly stabilizes the  $\kappa^3$  isomer ( $E(\kappa^2) - E(\kappa^3) = -20.5 \text{ kJ}\cdot\text{mol}^{-1}$ ). Adding the three contributions, considered as approximately independent, the higher stability of the  $\kappa^2$  isomer found without counteranion ( $-25.4 \text{ kJ}\cdot\text{mol}^{-1}$ ) is reversed, and the  $\kappa^3$  isomer becomes  $+1.4 \text{ kJ}\cdot\text{mol}^{-1}$  more stable, in agreement with what is found in the crystal structure. Although this analysis has only a semiquantitative value, it proves that in these cationic  $\text{Rh}^{\text{I}}$  complexes the counteranion does affect the preference for a coordination mode, and we can attribute to a counteranion effect the similar stabilities of the  $\kappa^2$  and  $\kappa^3$  isomers of  $[\text{Rh}(\text{N}_3^{\text{R}})\text{L}_2]^+$  complexes. A strong preference for the  $\kappa^2$  denticity can be envisaged for these  $\text{N}_3^{\text{R}}$  ligands in neutral complexes.

**$\kappa^3 \leftrightarrow \kappa^2$  Interconversion.** As summarized above, there is spectroscopic evidence for the interconversion of  $\kappa^2$  and  $\kappa^3$  isomers of  $[\text{Rh}(\text{N}_3^{\text{R}})\text{L}_2]^+$  complexes.<sup>2,3</sup> From a variable-temperature  $^1\text{H}$  NMR study on a mixture of the **1a** and **1b** isomers of  $[\text{Rh}(\text{N}_3^{\text{Me}})(\text{CO})_2]^+$  a  $\Delta G^\ddagger$  value of ca.  $70 \text{ kJ}\cdot\text{mol}^{-1}$  was estimated for the  $\kappa^3 \leftrightarrow \kappa^2 \leftrightarrow \kappa^3$  interconversion process. We have theoretically studied the  $\kappa^3 \leftrightarrow \kappa^2$  interconversion by searching for and locating the transition states that connect both minima for  $[\text{Rh}(\text{N}_3^{\text{Me}})\text{L}_2]^+$  ( $\text{L} = \text{cod}/2, \text{CO}$ ) systems. The main geometrical parameters of the transition states can be found in Table 4, and the transition state structures for the  $[\text{Rh}(\text{N}_3^{\text{Me}})\text{L}_2]^+$  complexes are depicted in Figure 6.

The mechanism for the  $\kappa^3 \leftrightarrow \kappa^2$  denticity changes of the  $\text{N}_3^{\text{R}}$  ligands can be deduced comparing the geometrical parameters of the transition states with those of the  $\kappa^3$  and  $\kappa^2$  minima. The process takes place in only one step, but involves simultaneous decoordination of the apical  $\text{N}_{\text{am}}$  ( $\text{Rh}-\text{N}_{\text{am}}$  distances of  $\sim 3.5 \text{ Å}$  in the transition states) and motion of the ethyl arm of the aminic nitrogen, as indicated by the trigonal planar  $\text{N}_{\text{am}}$  atom in the transition states (the sum of the three bond angles around the  $\text{N}_{\text{am}}$  atom is very close to  $360^\circ$ ). Thus, the theoretical study confirms the proposed mechanism with decoordination-inversion of the aminic nitrogen atom of the  $\text{N}$ -ligand for the  $\kappa^3 \leftrightarrow \kappa^2$  interconversion.

**Table 4. Energy Barriers, Relative to the  $\kappa^3$  Isomer, and Main Geometrical Parameters for the Transition States of the  $\kappa^3 \leftrightarrow \kappa^2$  Interconversion in  $[\text{Rh}(\text{N}_3^{\text{Me}})\text{L}_2]^+$  ( $\text{L} = \text{cod}/2, \text{CO}$ )<sup>a</sup>**

	$[\text{Rh}(\text{N}_3^{\text{Me}})(\text{cod})]^+$	$[\text{Rh}(\text{N}_3^{\text{Me}})(\text{CO})_2]^+$
$\Delta E^\ddagger$	+43.1	+65.4
$\Delta G^\ddagger$	+41.8	+52.1
Rh–L	2.078	1.893
L–L'	1.398	1.144
Rh–N <sub>pz</sub>	2.169	2.133
Rh–N <sub>am</sub>	3.493	3.455
L–Rh–L	86.8	92.2
N <sub>pz</sub> –Rh–N <sub>pz</sub>	81.2	82.5
N <sub>pz</sub> –Rh–L	96.1	92.6
$\Sigma \text{Rh}$	360.1	360.0
$\Sigma \text{N}_{\text{am}}$	353.7	359.5

<sup>a</sup> Distances are in Å, angles in deg, energies in  $\text{kJ}\cdot\text{mol}^{-1}$ .

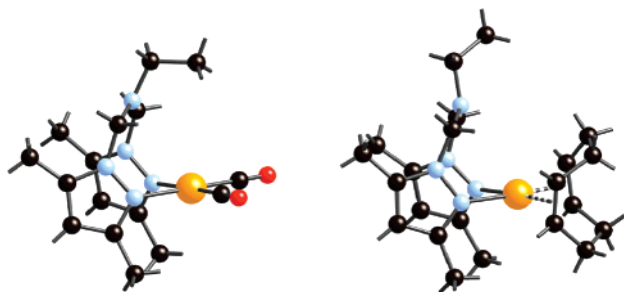


**Figure 6.** Transition states for the  $\kappa^3 \leftrightarrow \kappa^2$  isomerization of  $[\text{Rh}(\text{N}_3^{\text{Me}})(\text{CO})_2]^+$  (left) and  $[\text{Rh}(\text{N}_3^{\text{Me}})(\text{cod})]^+$  (right).

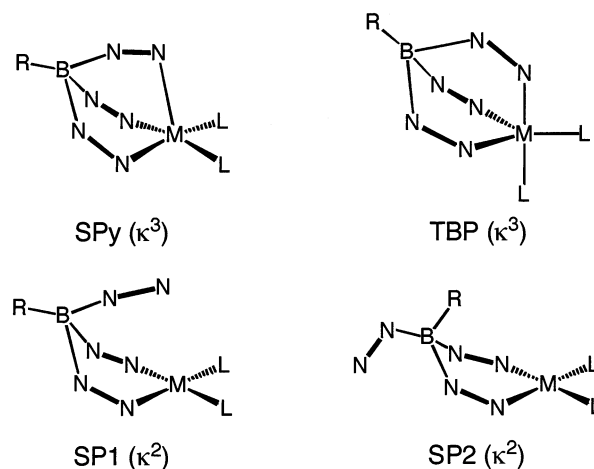
Energy barriers ( $\Delta E^\ddagger$ ) and activation free energies ( $\Delta G^\ddagger$ ) for the interconversion are given in Table 4. The  $\Delta G^\ddagger$  obtained from our calculations can be compared with the variable-temperature <sup>1</sup>H NMR measurement for the  $[\text{Rh}(\text{N}_3^{\text{Me}})(\text{CO})_2]^+$  complex. Our calculated values for this system (52 and 69  $\text{kJ}\cdot\text{mol}^{-1}$  for  $\kappa^3 \rightarrow \kappa^2$  and  $\kappa^2 \rightarrow \kappa^3$  reactions, respectively) are in good agreement with the experimental data ( $\Delta G^\ddagger$  of 70  $\text{kJ}\cdot\text{mol}^{-1}$ ).<sup>3</sup> The range of the energy barriers obtained is consistent with the process of inversion of configuration of a  $\text{NR}_3$  group taking place.<sup>18</sup> Similar activation parameters have been reported for  $[\text{Rh}(\text{cod})]^+$  and  $[\text{Ir}(\text{cod})]^+$  complexes with  $\kappa^3$ -(amine)(pyridine)<sub>2</sub> ligands having  $\text{N}_{\text{am}}\text{--CH}_2\text{--N}_{\text{py}}$  linkers ( $\Delta G^\ddagger \approx 63$  and  $67 \text{ kJ}\cdot\text{mol}^{-1}$  and  $\Delta H^\ddagger \approx 50$  and  $59 \text{ kJ}\cdot\text{mol}^{-1}$  for the Rh and Ir complexes, respectively),<sup>6</sup> in which other dynamic processes involving the diene ligands present higher energies. A very close value of  $\sim 61 \text{ kJ}\cdot\text{mol}^{-1}$  has been found for the same denticity changes observed in similar palladium compounds such as  $\text{PdCl}_2$ ,  $[\text{PdMe}(\text{NCMe})]^+$ , and  $[\text{PdMe}(\text{C}_2\text{H}_4)]^+$  with multidentate *N*-donor ligands in which the hapticity change implies the inversion of the aminic nitrogen.<sup>14</sup> On the contrary, when the decoordination process is not accompanied by the nitrogen inversion, as in  $[\text{RhCl}(\text{py}^{\text{Me}}\text{--CH=NR})(\text{nbd})]$ , a lower value of about 40  $\text{kJ}\cdot\text{mol}^{-1}$  has been reported.<sup>19</sup>

Although all the calculated energy barriers for the  $\kappa^3 \leftrightarrow \kappa^2$  interconversion are in the same range, our results show lower barriers for complexes having cyclooctadiene ligands than for the carbonyl ones (between 13 and 23  $\text{kJ}\cdot\text{mol}^{-1}$  lower). This trend can be related to the higher

stabilization of the  $\kappa^3$  coordination mode in the carbonyl compounds.

**Comparison with Other *N*-Ligands.** The most well-developed pyrazole-based ligands are the poly-(pyrazolyl)borates and related ligands known as scorpionates.<sup>10,11</sup> A large amount of structural information obtained by X-ray diffraction, <sup>13</sup>C, <sup>15</sup>N, <sup>103</sup>Rh, and <sup>11</sup>B NMR chemical shifts, or IR stretching frequencies of C–O and B–H bonds can be used to assign the hapticity of the scorpionates.<sup>20</sup> The great amount of chemical information available for these species will be very useful for us to compare with the  $\text{N}_3^{\text{R}}$  compounds studied here. When a scorpionate acts as a ligand on a  $d^8$  transition metal, in addition to the well-known tridentate  $\kappa^3\text{--N,N',N''}$  and bidentate  $\kappa^2\text{--N,N'}$  binding modes,<sup>21</sup> new modes have been recently discovered as monodentate  $\kappa^1\text{--N}$ ,<sup>22</sup> uncoordinated counteranion (i.e.,  $\kappa^0$ ),<sup>23</sup> or involving agostic B–H $\cdots$ M interaction.<sup>24</sup>

The X-ray structures of  $d^8\text{--}[\text{M}(\text{Tp}^{\text{R}})\text{L}_2]$  where  $\text{Tp}^{\text{R}}$  is hydridotris(1-pyrazolyl)borate, can be classified according to four basic geometries (2):<sup>25</sup>



2

two square-planar (SP) geometries with an uncoordinated third pyrazolyl nitrogen (one with the uncoordinated third pyrazolyl arm over the square-plane (SP1), and the other with an “inverted” boron (SP2)), a trigonal bipyramidal (TBP) geometry with a  $\kappa^3$ -Tp, and a square-pyramidal (SPy) geometry with the third pyrazolyl arm at an intermediate coordination with a long M–N bond. Each kind of structure can be stabilized by selecting a determined R-substituent for  $\text{Tp}^{11,26,27}$  or L

(20) Slugovc, C.; Padilla-Martínez, I.; Sirol, S.; Carmona, E. *Coord. Chem. Rev.* **2001**, *213*, 129.

(21) Edelmann, F. T. *Angew. Chem., Int. Ed.* **2001**, *40*, 1656.

(22) Paneque, M.; Sirol, S.; Trujillo, M.; Gutiérrez-Puebla, E.; Monge, M. A.; Carmona, E. *Angew. Chem., Int. Ed.* **2000**, *39*, 218.

(23) Paneque, M.; Sirol, S.; Trujillo, M.; Carmona, E.; Gutiérrez-Puebla, E.; Monge, M. A.; Ruiz, C.; Malbosc, F.; Serra-Le Berre, C.; Kalck, P.; Etienne, M.; Daran, J.-C. *Chem. Eur. J.* **2001**, *7*, 3869.

(24) Herberhold, M.; Eibl, S.; Milius, W.; Wrackmeyer, B. *Z. Anorg. Allg. Chem.* **2000**, *626*, 552.

(25) A search in the Cambridge Structural Database for rhodium-(I) scorpionate complexes shows 65 independent structures having only 12 for the SPy ( $\kappa^3$ ) isomer. The rest are 35 for SP1, 3 for SP2, and 15 for TBP (see Supporting Information).

(26) Adams, C. J.; Connelly, N. G.; Emslie, D. J. H.; Hayward, O. D.; Manson, T.; Orpen, A. G.; Rieger, P. H. *Dalton Trans.* **2003**, 2835.

(27) Connelly, N. G.; Emslie, D. J. H.; Geiger, W. E.; Hayward, O. D.; Linehan, E. B.; Orpen, A. G.; Quayle, M. J.; Rieger, P. H. *J. Chem. Soc., Dalton Trans.* **2001**, 670.

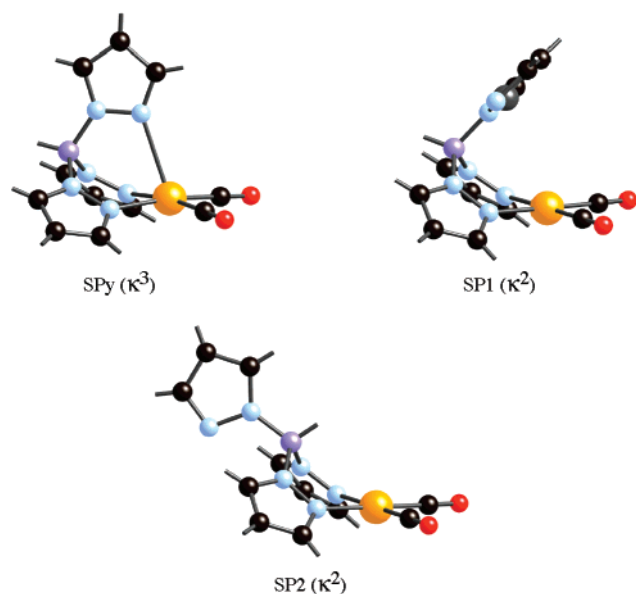
(18) Günther, H. *NMR Spectroscopy*; John Wiley & Sons: New York, 1980.

(19) Haarman, H. F.; Bregman, F. R.; Ernsting, J.-M.; Veldman, N.; Spek, A. L.; Vrieze, K. *Organometallics* **1997**, *16*, 54.

**Table 5. Optimized Structural Parameters for the  $\kappa^2$  and  $\kappa^3$  Isomers of  $[\text{Rh}(\text{Tp}^R)(\text{CO})_2]$  ( $R = \text{H}, \text{Me}$ )<sup>a</sup>**

parameter <sup>b</sup>	$[\text{Rh}(\text{Tp}^H)(\text{CO})_2]$			$[\text{Rh}(\text{Tp}^{\text{Me}})(\text{CO})_2]$		
	SPy ( $\kappa^3$ )	SP1 ( $\kappa^2$ )	SP2 ( $\kappa^2$ )	SPy ( $\kappa^3$ )	SP1 ( $\kappa^2$ ) <sup>d</sup>	SP2 ( $\kappa^2$ )
Rh–C	1.876	1.885	1.886	1.874	1.884	1.884
C–O	1.150	1.148	1.148	1.152	1.149	1.149
Rh–N <sub>bs</sub>	2.136	2.109	2.107	2.143	2.110	2.109
Rh–N <sub>ap</sub>	2.743	~3.8 <sup>c</sup>	5.605	2.615	~3.8 <sup>c</sup>	5.615
L–Rh–L	91.5	92.1	92.4	90.0	91.4	91.6
N <sub>bs</sub> –Rh–N <sub>bs</sub>	86.2	87.0	86.6	84.2	85.3	84.4
N <sub>bs</sub> –Rh–L	90.7	90.4	90.5	92.5	91.6	92.0
N <sub>ap</sub> –Rh–N <sub>bs</sub>	80.1			83.2		
N <sub>ap</sub> –Rh–L	106.2			103.0		
∑Rh	359.2	360.0	360.0	359.2	360.0	360.0

<sup>a</sup> Distances are in Å, angles in deg. <sup>b</sup> N<sub>bs</sub> and N<sub>ap</sub> are basal and apical nitrogen atoms. <sup>c</sup> Distance between the rhodium atom and the centroid of the pyrazolyl ring (the torsion angle Rh–B–C–N<sub>ap</sub> is 87.2°). <sup>d</sup> Not a minimum; the torsion angle Rh–B–C–N<sub>ap</sub> is fixed at the value found for the R = H analogue (87.2°).

**Figure 7.** Optimized structures of the  $\kappa^3$  and  $\kappa^2$  isomers of  $[\text{Rh}(\text{Tp}^H)(\text{CO})_2]$ .

ligands.<sup>26,28</sup> Very recently the SPy, SP1, and SP2 forms of  $[\text{Rh}(\text{Tp}^{3-R})(\text{CO})_2]$  ( $R = p\text{-C}_6\text{H}_4\text{Cl}$ ) have been isolated and characterized by X-ray diffraction.<sup>29</sup> To our knowledge, this is the only compound with a ( $\text{Tp}^R$ ) ligand that has been isolated and characterized in more than one isomeric form. A thorough theoretical study on the factors affecting the structure and relative energy of various isomers of  $\text{Tp}^R$  rhodium(I) dicarbonyl complexes and their interconversion pathway has been published recently.<sup>30</sup>

Aiming to compare the behavior of  $[\text{Rh}(\text{N}_3^R)\text{L}_2]^+$  complexes with those with  $\text{Tp}^R$  ligands we have optimized the SP1, SP2, and SPy isomers of  $[\text{Rh}(\text{Tp}^R)(\text{CO})_2]$  ( $R = \text{H}, \text{Me}$ ) complexes. The optimized geometries for  $R = \text{H}$  are drawn in Figure 7. The structural parameters are given in Table 5. Our results are in good agreement with those previously reported.<sup>30</sup> SP1 and SP2 complexes present basically the same geometry for the four basal ligands,<sup>30,31</sup> two L donors and two pyrazolyl rings

(28) (a) Ohta, K.; Hashimoto, M.; Takahashi, Y.; Hikichi, S.; Akita, M.; Moro-oka, Y. *Organometallics* **1999**, *18*, 3234. (b) Akita, M.; Hashimoto, M.; Hikichi, S.; Moro-oka, Y. *Organometallics* **2000**, *19*, 3744.

(29) Criado, R.; Cano, M.; Campo, J. A.; Heras, J. V.; Pinilla, E.; Torres, M. R. *Polyhedron* **2004**, *23*, 301.

(30) Webster, C. E.; Hall, M. B. *Inorg. Chim. Acta* **2002**, *330*, 268.

**Table 6. Calculated Relative Energies (in  $\text{kJ}\cdot\text{mol}^{-1}$ ) of the  $\kappa^2$  and  $\kappa^3$  Isomers of  $[\text{Rh}(\text{Tp}^R)(\text{CO})_2]$  ( $R = \text{H}, \text{Me}$ )<sup>a</sup>**

compound	isomer			reference
	SPy ( $\kappa^3$ )	SP1 ( $\kappa^2$ )	SP2 ( $\kappa^2$ )	
R = H	0.0	+14.7 (–10.5)	+2.8 (–14.7)	this work
	0.0	+15.0	+3.3	ref 30
R = Me	0.0	+10.2 <sup>b</sup> (–17.7)	+26.4 (+10.4)	this work
	0.0	+12.5	+31.8	ref 30

<sup>a</sup> In parentheses is given the relative energy of the free ligand, calculated at the geometry that it adopts in the  $\kappa^2$  and  $\kappa^3$  isomer of each complex. <sup>b</sup> Not a minimum; the torsion angle Rh–B–C–N<sub>ap</sub> is fixed at the value found for the R = H analogue.

attached directly to rhodium: it is worth mentioning that although the SP1 isomers of  $\text{Tp}^R$  complexes are usually described as  $\kappa^2$  systems, with a noninteracting third pyrazolyl ring, the distances Rh–centroid(pz) found (about 3.8 Å)<sup>32</sup> may indicate the existence of a stacking interaction between the  $\pi$  system of this third pyrazolyl ring and the rhodium atom. This possibility, which deserves further exploration, is not possible with the  $\text{N}_3^R$  ligands, in which the third arm is of aminic character.

The main structural difference observed in the  $\text{Tp}^R$  complexes (Table 5) from the related  $\text{N}_3^R$  complexes (Table 1) is the 0.1 Å shorter Rh–N apical bond lengths found in the  $\kappa^3$  isomers of Tp compounds, due to the better orientation of the N-donor atom lone pair.<sup>13</sup> On the contrary, no difference can be found for basal bond lengths. The same trends are observed in  $\text{Tp}^R$  and  $\text{N}_3^R$  ligands when methyl groups are introduced in the 3 and 5 positions of the pyrazolyl rings: the lengthening of basal and the shortening of apical Rh–N bond distances and the decrease of the N<sub>bs</sub>–Rh–N<sub>bs</sub> bond angles.<sup>30</sup>

The relative energies of the different isomers of  $[\text{Rh}(\text{Tp}^R)(\text{CO})_2]$  ( $R = \text{H}, \text{Me}$ ) are collected in Table 6. The stability order found for the isomers of the unsubstituted  $\text{Tp}^H$  ligands is SPy ( $\kappa^3$ )  $\geq$  SP2 ( $\kappa^2$ ) > SP1 ( $\kappa^2$ ), although the energy differences between them are small. Methyl substitution destabilizes the SP2 structure, due to steric interactions with the uncoordinated pyrazolyl arm. Although the energy of the SP1 structure is close to the SPy one, it is not a minimum and evolves to the  $\kappa^3$  one by rotating  $\sim 90^\circ$  around the B–C<sub>pz</sub> bond. Our results are in good agreement with the theoretical values

(31) Bucher, U. E.; Currao, A.; Nesper, R.; Rügger, H.; Venanzi, L. M.; Younger, E. *Inorg. Chem.* **1995**, *34*, 66.

(32) Malbosc, F.; Chauby, V.; Serra-Le Berre, C.; Etienne, M.; Daran, J.-C.; Kalk, P. *Eur. J. Inorg. Chem.* **2001**, 2689.

previously reported<sup>30</sup> and also agree with the experimental results showing that two isomers can separately crystallize.<sup>29</sup> The calculated energy differences between the SPy ( $\kappa^3$ ) and SP1 ( $\kappa^2$ ) forms of  $[\text{Rh}(\text{Tp}^R)(\text{CO})_2]$  complexes (14.7  $\text{kJ}\cdot\text{mol}^{-1}$  with  $\text{Tp}^H$  and 10.2  $\text{kJ}\cdot\text{mol}^{-1}$  with  $\text{Tp}^{\text{Me}}$  ligands, respectively) agree with the  $\Delta H^\circ$  of 12.3  $\text{kJ}\cdot\text{mol}^{-1}$  estimated by spectroscopic methods for  $[\text{Rh}(\text{Tp}^{\text{Ph}})(\text{CO})_2]$ .<sup>11</sup>

The comparison of the relative energies of the different isomers for complexes  $[\text{Rh}(\text{N}_3^R)\text{L}_2]^+$  (Table 3) and  $[\text{Rh}(\text{Tp}^R)\text{L}_2]$  (Table 6) shows important differences. The main difference is that with  $\text{Tp}^R$  ligands  $\kappa^3$  and  $\kappa^2$  energies are much closer, the SPy ( $\kappa^3$ ) structures being slightly more stable than the  $\kappa^2$  ones, as found in the previous study.<sup>30</sup> As pointed out above, shorter Rh–N apical bond distances are found in  $[\text{Rh}(\text{Tp}^R)\text{L}_2]$  complexes than in  $[\text{Rh}(\text{N}_3^R)\text{L}_2]^+$  ones, due to a better orientation of the lone pair of the third nitrogen atom. Consequently, the great stability of  $\kappa^3$  isomers could be assigned to the formation of a stronger apical bond. However, there is another factor accounting for the preference of  $\text{Tp}^R$  ligands for the  $\kappa^3$  coordination mode: the intrinsic greater stability of the ligand in the conformation it adopts in this coordination mode. As for the  $\text{N}_3^R$  ligands, we have calculated the energy of the free  $\text{Tp}^R$  ligands, at the geometry that they adopt in both the  $\kappa^2$  and  $\kappa^3$  isomers of each complex (Table 6, values in parentheses). Comparing the energy difference between the two forms of the free ligands, we can conclude that the  $\text{Tp}^R$  always prefers the conformation it adopts in a  $\kappa^2$  coordination mode, although the energy differences between the two forms are smaller than for the  $\text{N}_3^R$ . The interaction of the ligand with the  $\{\text{Rh}(\text{CO})_2\}$  fragment decreases this preference by 17 and 26  $\text{kJ}\cdot\text{mol}^{-1}$  for the SP2 and SP1 structures, respectively, with almost no influence of the R substituent. The higher interaction value found for the SP1 structures could be a further indication of the existence of a stabilizing interaction between the metal atom and the  $\pi$  system of the third pyrazolyl ring of the  $\text{Tp}^R$  ligand.

A fast exchange of the pyrazolyl ring is observed in solution for most of the  $[\text{Rh}(\text{Tp}^R)\text{L}_2]$  complexes, which includes a  $\kappa^3 \leftrightarrow \kappa^2$  equilibrium.<sup>28,30–32</sup>  $\Delta G^\ddagger$  data for this exchange have been estimated from the NMR coalescence temperatures. Values of about 46  $\text{kJ}\cdot\text{mol}^{-1}$  have been obtained for scorpionates with nonsubstituted pyrazolyl rings.<sup>33,34</sup> The values increase to 63–77  $\text{kJ}\cdot\text{mol}^{-1}$  for complexes with bulky ligands.<sup>33</sup> Given that the interconversion between  $\kappa^3$  and  $\kappa^2$  coordination modes of the  $\text{Tp}^R$  ligands takes place with a coordination–rotation–recoordination process, without nitrogen inversion, lower barriers than for related  $[\text{Rh}(\text{N}_3^R)\text{L}_2]$  compounds are found.

From the small energy differences found between the five- and four-coordinate isomers of  $\text{Rh}^I$  complexes with  $\text{Tp}^R$  ligands, a high flexibility in the coordination mode of these ligands can be expected, with a broad distribution of the experimental structures between the possible geometries. We have retrieved from the Cambridge Structural Database (see Supporting Information) complexes with general formulas  $[\text{M}(\text{REp}_3)\text{L}_2]$  and

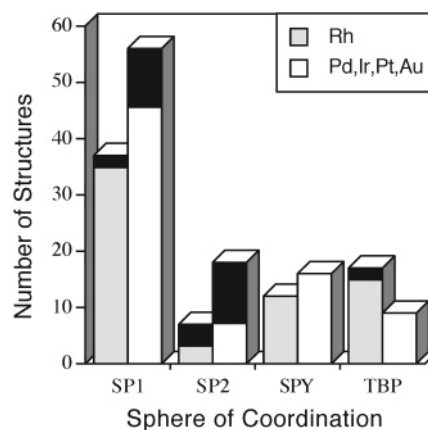


**Figure 8.** Distribution of the molecular structures of  $d^8$ - $[\text{M}(\text{Tp}^R)\text{L}_2]$  complexes from the Cambridge Structural Database.  $\text{Rh}^I$  compounds are separated from other  $d^8$  transition metals such as  $\text{Ir}^I$ ,  $\text{Pd}^{II}$ ,  $\text{Pt}^{II}$ , and  $\text{Au}^{III}$  (see Supporting Information for data). Black bars show the compounds in which  $\text{Epz}_4$  is the  $\text{Tp}$  ligand (see text). The molecular structures are drawn in 2.

$[\text{M}(\text{Epz}_4)\text{L}_2]$  in which M is a  $d^8$  transition metal such as  $\text{Rh}^I$ ,  $\text{Pd}^{II}$ ,  $\text{Ir}^I$ ,  $\text{Pt}^{II}$ , and  $\text{Au}^{III}$  (having 60, 46, 7, 15, and 7 compounds, respectively). We have not considered the related  $\text{Ni}^{II}$  complexes (62 compounds) due to their tendency to present hexacoordinate structures. These structures are classified depending on the role of the third pyrazolyl ring in the coordination sphere of the transition metal according to the basic geometries ( $\kappa^2$ : SP1 and SP2;  $\kappa^3$ : TBP and SPy). The distribution of molecular structures for  $d^8$ - $[\text{M}(\text{Tp}^R)\text{L}_2]$  complexes is depicted in Figure 8. Notice that complexes  $[\text{M}(\text{Epz}_4)\text{L}_2]$  count twice for the third and fourth pyrazolyl rings. For comparative purposes  $\text{Rh}^I$  compounds are separated from the other  $d^8$  transition metal compounds. As expected from the structural flexibility of  $\text{Tp}^R$  ligands, all four structural classes are populated. Figure 8 shows that a very similar distribution is found for rhodium(I) and for the other  $d^8$  ions. The coordination mode of the  $\text{Tp}^R$  ligand in these  $d^8$  compounds appears as mainly independent of the transition metal M nature. This result agrees with the similar stability found for related iridium(I) and rhodium(I) complexes.<sup>30</sup> For the  $\kappa^2$  coordination mode the analysis reveals the great structural preference for the SP1 isomer and the poor tendency for the SP2 form. In fact the SP1 class is the most populated group. For the  $\kappa^3$  hapticity, a similar structural characterization of trigonal-bipyramid and square-pyramid geometries is found, although the SPy structure is clearly preferred by oxidation of rhodium(I) to rhodium(II).<sup>26,27,35</sup> However, the TBP structure has been characterized as a low lying transition state in the case of rhodium(I) dicarbonyl complexes.<sup>30</sup>

## Conclusions

In the present work we have extended the study of the hapticity of (amine)(pyrazole)<sub>2</sub> three-*N*-donor ligands ( $\text{N}_3^R$ ) to the simplest bis(1-pyrazolylmethyl)ethylamine ligand, in which no substituents are present in the pyrazolyl ring. As for the previous methyl-substituted

(33) Kläui, W.; Schramm, D.; Peters, W.; Rheinwald, G.; Lang, H. *Eur. J. Inorg. Chem.* **2001**, 1415.

(34) Ruman, T.; Ciunik, Z.; Trzeciak, A. M.; Wolowicz, S.; Ziolkowski, J. *J. Organometallics* **2003**, *22*, 1072.

(35) Geiger, W. E.; Ohrenberg, N. C.; Yeomans, B.; Connelly, N. G.; Emslie, D. J. *J. Am. Chem. Soc.* **2003**, *125*, 8680.



compounds, both the dicarbonyl and cyclooctadiene rhodium(I) complexes present an equilibrium in solution between the  $\kappa^2$  and  $\kappa^3$  isomers. The square-pyramidal  $\kappa^3$  structures are strongly favored by the presence of carbonyl ligands and to a lesser extent by the methyl substituents in the *N*-ligand. We have theoretically analyzed the coordination mode of  $N_3^R$  ligands in  $[\text{Rh}(\text{N}_3^R)\text{L}_2]^+$  ( $\text{L} = \text{cod}/2$ ,  $\text{CO}$ ;  $\text{R} = \text{H}$ ,  $\text{Me}$ ) complexes. Both the  $\kappa^2$ -(pyrazole)<sub>2</sub> and  $\kappa^3$ -(amina)(pyrazole)<sub>2</sub> isomers have been found as minima. The optimized structural parameters are in good agreement with the available experimental data.

Although the experimental stability trends for  $\kappa^2$  and  $\kappa^3$  forms are reproduced by calculations of only the  $[\text{Rh}(\text{N}_3^R)\text{L}_2]^+$  cationic part of the complex, pentacoordinate complexes being more stable for carbonyl ligands and *N*-methyl-substituted pyrazol rings than for cyclooctadiene and nonsubstituted ones, these calculations fail in correctly reproducing the experimental preference for the  $\kappa^3$  coordination mode. There is a strong intrinsic preference for the ligand to adopt the conformation found in  $\kappa^2$  compounds, which cannot be reversed by coordination to the  $\{\text{RhL}_2\}$  metal fragment. However, the rhodium(I) complexes considered are cationic, and a counteranion is always present. Introduction of a  $[\text{BF}_4]^-$  in the calculations shows that the  $\text{Rh}\cdots\text{B}$  distances, and as a consequence the  $\kappa^2$  and  $\kappa^3$  relative energies in two of the three regions where the anion can be placed, are considerably affected by the change in the coordination mode. The stronger interaction of  $[\text{Rh}(\text{N}_3^R)\text{L}_2]^+$  with the  $[\text{BF}_4]^-$  counteranion in the  $\kappa^3$  isomer appears as the main reason responsible for the solid state preference for the  $\kappa^3$  coordination mode and the very similar energies of both isomers in solution. Thus, this study proves that counterion effects can be very important in determining the hapticity of a multidentate ligand in a cationic complex.

The  $\kappa^3 \leftrightarrow \kappa^2$  interconversion has also been studied. A transition state for the dynamic process has been determined and characterized, which agrees with a mechanism implying an inversion of configuration at the aminic nitrogen atom. The calculated barriers are in good agreement with the experimental data. A higher energy barrier is found for the carbonyl complexes than the cyclooctadiene  $\kappa^3$  ones, in agreement with the greater preference of carbonyl compounds for the  $\kappa^3$  coordination mode.

To relate the behavior of our  $N_3^R$  ligands with other ligands with three *N*-donor atoms, we have carried out a theoretical study for analogous compounds having  $\text{Tp}^R$  scorpionates as *N*-ligands. The main structural difference found in  $[\text{Rh}(\kappa^3\text{-Tp}^R)(\text{CO})_2]$  complexes with respect to  $\kappa^3\text{-N}_3^R$  is the shorter  $\text{Rh}-\text{N}$  distance for the apical ligand, which can be attributed to the better donor properties of the *N*-lone pair. The energies of isomers  $\kappa^3$  and  $\kappa^2$  are much closer in  $\text{Tp}^R$ -containing compounds, the  $\kappa^3$  square-pyramidal structures being slightly more stable than the  $\kappa^2$  ones. The ligands show an intrinsic preference for the conformation they adopt in the  $\kappa^3$  coordination mode. The small energy differences found between the five- and four-coordinate isomers of  $\text{Rh}^I$  complexes with  $\text{Tp}^R$  ligands agree with the high coordinative flexibility of the (pyrazole)<sub>3</sub> ligands, as proved by a structural analysis of the X-ray structures of

$d^8\text{-}[\text{M}(\text{Tp}^R)\text{L}_2]$  complexes from the Cambridge Structural Database.

## Experimental Section

**General Remarks.** All reactions were performed under a nitrogen atmosphere with the use of standard Schlenk techniques. Tetrahydrofuran and diethyl ether used for the synthesis were distilled under nitrogen from sodium benzophenone ketyl just before use. Other solvents were purified following the standard procedures and stored under nitrogen. NMR spectra were recorded on a Bruker AC 250 instrument. All chemical shift values are given in ppm and are referenced with respect to residual protons in the solvent for proton spectra and to solvent signals for <sup>13</sup>C spectra. Elemental analyses were performed in our laboratory on a Perkin-Elmer 2400 CHN analyzer. The bis(1-pyrazolylmethyl)ethylamine<sup>12</sup> and  $[\text{Rh}_2\text{Cl}_2(\text{cod})_2]$ <sup>36</sup> have been prepared according to published procedures.

**Synthesis of  $[\text{Rh}(\text{N}_3^H)(\text{cod})][\text{BF}_4]$ .** To a solution of 0.079 g (0.16 mmol) of  $[\text{Rh}_2\text{Cl}_2(\text{cod})_2]$  in 20 mL of thf was added 0.062 g (0.32 mmol) of  $\text{AgBF}_4$ , and the solution was stirred for half an hour at room temperature. The orange solution turned yellow and  $\text{AgCl}$  precipitated. The solution was then filtered through a pad of Celite, and 0.066 g (0.32 mmol) of  $\text{N}_3^H$  was then added. After stirring for an hour, the solution was evaporated to dryness and the residue was crystallized in a dichloromethane/ether mixture to give 0.141 g (87%) of  $[\text{Rh}(\text{N}_3^H)(\text{cod})][\text{BF}_4]$  as yellow crystals.

Anal. Calcd for  $\text{C}_{18}\text{H}_{27}\text{BF}_4\text{N}_5\text{Rh}$ : C, 42.97; H, 5.41; N, 13.92. Found: C, 43.01; H, 5.29; N, 13.78. Isomer  $\kappa^2$ : <sup>1</sup>H NMR ( $\text{CDCl}_3$  solution, 250 MHz,  $\delta$ ): 7.70 (s, 2H, CH pyrazole); 7.60 (s, 2H, CH pyrazole); 6.45 (d, <sup>2</sup>J = 15.1 Hz, 2H,  $\text{CH}_2\text{N}$ ); 6.24 (s, 2H, CH middle pyrazole); 5.60 (d, <sup>2</sup>J = 15.1 Hz, 2H,  $\text{CH}_3\text{N}$ ); 4.15 (b, 4H, CH cod); 2.69 (b, 8H,  $\text{CH}_2$  cod); 2.01 (q, <sup>3</sup>J = 7.0 Hz, 2H,  $\text{CH}_2\text{CH}_3$ ); 1.10 (t, <sup>3</sup>J = 7.0 Hz, 3H,  $\text{CH}_2\text{CH}_3$ ). <sup>13</sup>C{<sup>1</sup>H} NMR ( $\text{CDCl}_3$  solution, 63 MHz,  $\delta$ ): 141.2 (CH pyrazole); 134.0 (CH pyrazole); 108.2 (CH middle pyrazole); 86.9–84.3 (m, =CH cod); 71.4 ( $\text{CH}_2\text{N}$ ); 42.3 ( $\text{CH}_2\text{CH}_3$ ); 31.3–30.5 ( $\text{CH}_2$  cod); 12.4 ( $\text{CH}_2\text{CH}_3$ ). Isomer  $\kappa^3$ : <sup>1</sup>H NMR ( $\text{CDCl}_3$  solution, 250 MHz,  $\delta$ ): 7.70 (s, 2H, CH pyrazole); 7.60 (s, 2H, CH pyrazole); 6.11 (s, 2H, CH middle pyrazole); 5.17 (s, 4H,  $\text{CH}_2\text{N}$ ); 3.92 (b, 4H, CH cod), 2.57 (b, 8H,  $\text{CH}_2$  cod); 1.85 (q, <sup>3</sup>J = 6.9 Hz, 2H,  $\text{CH}_2\text{CH}_3$ ); 1.53 (t, <sup>3</sup>J = 6.9 Hz, 3H,  $\text{CH}_2\text{CH}_3$ ). <sup>13</sup>C{<sup>1</sup>H} NMR ( $\text{CDCl}_3$  solution, 63 MHz,  $\delta$ ): 142.4 (CH pyrazole); 133.5 (CH pyrazole); 107.7 (CH middle pyrazole); 86.9–84.3 (m, =CH cod); 68.8 ( $\text{CH}_2\text{N}$ ); 52.6 ( $\text{CH}_2\text{CH}_3$ ); 31.3–30.5 ( $\text{CH}_2$  cod); 11.6 ( $\text{CH}_2\text{CH}_3$ ).

**Synthesis of  $[\text{Rh}(\text{N}_3^H)(\text{CO})_2][\text{BF}_4]$ .** Carbon monoxide was bubbled for 1 h in a solution of 0.141 g (0.28 mmol) of  $[\text{Rh}(\text{N}_3^H)(\text{cod})][\text{BF}_4]$  dissolved in 20 mL of dichloromethane. The solution was then evaporated to dryness in a vacuum, leaving 0.080 g (78%) of  $[\text{Rh}(\text{N}_3^H)(\text{CO})_2][\text{BF}_4]$  as a yellow powder.

Anal. Calcd for  $\text{C}_{12}\text{H}_{15}\text{BF}_4\text{N}_5\text{O}_2\text{Rh}$ : C, 31.96; H, 3.35; N, 15.53. Found: C, 32.25; H, 3.24; N, 15.24. IR ( $\text{CH}_2\text{Cl}_2$  solution,  $\nu_{\text{CO}}$ ): 2109 (s), 2088 (s), 2049 (s), 2021 (s)  $\text{cm}^{-1}$ . Isomer  $\kappa^2$ : <sup>1</sup>H NMR ( $\text{CDCl}_3$  solution, 250 MHz,  $\delta$ ): 7.68 (s, 2H, CH pyrazole); 7.60 (s, 2H, CH pyrazole); 6.49–5.25 (m, 4H,  $\text{CH}_2\text{N}$ ); 6.39 (s, 2H, CH middle pyrazole); 2.04 (q, <sup>3</sup>J = 6.9 Hz, 2H,  $\text{CH}_2\text{CH}_3$ ); 1.27 (t, <sup>3</sup>J = 6.9 Hz, 3H,  $\text{CH}_2\text{CH}_3$ ). <sup>13</sup>C{<sup>1</sup>H} NMR ( $\text{CDCl}_3$  solution, 63 MHz,  $\delta$ ): 183.2–180.5 (CO); 136.7–128.9 (CH pyrazole); 108.9 (CH middle pyrazole); 74.4 ( $\text{CH}_2\text{N}$ ); 40.4 ( $\text{CH}_2\text{CH}_3$ ); 12.2 ( $\text{CH}_2\text{CH}_3$ ). Isomer  $\kappa^3$ : <sup>1</sup>H NMR ( $\text{CDCl}_3$  solution, 250 MHz,  $\delta$ ): 7.68 (s, 2H, CH pyrazole); 7.60 (s, 2H, CH pyrazole); 6.49–5.25 (m, 4H,  $\text{CH}_2\text{N}$ ); 6.35 (s, 2H, CH middle pyrazole); 3.01 (q, <sup>3</sup>J = 6.9 Hz, 2H,  $\text{CH}_2\text{CH}_3$ ); 1.37 (t, <sup>3</sup>J = 6.9 Hz, 3H,  $\text{CH}_2\text{CH}_3$ ). <sup>13</sup>C{<sup>1</sup>H} NMR ( $\text{CDCl}_3$  solution, 63 MHz,  $\delta$ ): 183.2–180.5 (CO); 136.7–128.9 (CH pyrazole); 108.7 (CH middle pyrazole); 68.6 ( $\text{CH}_2\text{N}$ ); 48.3 ( $\text{CH}_2\text{CH}_3$ ); 11.5 ( $\text{CH}_2\text{CH}_3$ ).

**Computational Details.** DFT calculations were carried out using the GAUSSIAN98 package.<sup>37</sup> The hybrid B3LYP functional was applied.<sup>38</sup> Effective core potentials (ECP) were used to represent the innermost electrons of the rhodium atom.<sup>39</sup> The basis set for the Rh atom was that associated with the pseudopotential,<sup>39</sup> with a standard double- $\zeta$  LANL2DZ contraction.<sup>37</sup> The basis set for the main group elements was 6-31G,<sup>40</sup> having an extra polarization function (6-31G\*)<sup>41</sup> for the atoms directly attached to the metal (three *N*-donor atoms in all isomers, C of the coordinated olefin and carbonyl, and also O of carbonyl ligands). The geometries were fully optimized using gradient techniques. The transition states were characterized by a vibrational analysis. To account for the counteranion effect, the energy of the  $[Rh(N_3^{M_e})(cod)]^+[BF_4]^-$  ion pair was calculated for the  $\kappa^2$  and  $\kappa^3$  isomers, with the  $BF_4^-$

(37) Frisch, M. J.; Trucks, G. W.; Schlegel, H. B.; Scuseria, G. E.; Robb, M. A.; Cheeseman, J. R.; Zakrzewski, V. G.; Montgomery, J. A.; Stratmann, R. E.; Burant, J. C.; Dapprich, S.; Millam, J. M.; Daniels, A. D.; Kudin, K. N.; Strain, M. C.; Farkas, O.; Tomasi, J.; Barone, V.; Cossi, M.; Cammi, R.; Mennucci, B.; Pomelli, C.; Adamo, C.; Clifford, S.; Ochterski, J.; Petersson, G. A.; Ayala, P. Y.; Cui, Q.; Morokuma, K.; Malick, D. K.; Rabuck, A. D.; Raghavachari, K.; Foresman, J. B.; Cioslowski, J.; Ortiz, J. V.; Stefanov, B. B.; Liu, G.; Liashenko, A.; Piskorz, P.; Komaromi, I.; Gomperts, R.; Martin, R. L.; Fox, D. J.; Keith, T.; Al-Laham, M. A.; Peng, C. Y.; Nanayakkara, A.; Gonzalez, C.; Challacombe, M.; Gill, P. M. W.; Johnson, B.; Chen, W.; Wong, M. W.; Andres, J. L.; Gonzalez, C.; Head-Gordon, M.; Replogle, E. S.; Pople, J. A. *Gaussian 98 (Revision A.7)*; Gaussian Inc.: Pittsburgh, PA, 1998.

(38) (a) Becke, A. D. *J. Chem. Phys.* **1993**, *98*, 5648. (b) Lee, C.; Yang, W.; Parr, R. G. *Phys. Rev. B* **1988**, *37*, 785.

(39) Hay, P. J.; Wadt, W. R. *J. Chem. Phys.* **1985**, *82*, 299.

(40) Hehre, W. J.; Ditchfield, R.; Pople, J. A. *J. Chem. Phys.* **1972**, *56*, 2257.

(41) (a) Hariharan, P. C.; Pople, J. A. *Theor. Chim. Acta* **1973**, *28*, 213. (b) Francl, M. M.; Pietro, W. J.; Hehre, W. J.; Binkley, J. S.; Gordon, M. S.; Defrees, D. J.; Pople, J. A. *J. Chem. Phys.* **1982**, *77*, 3654.

placed in five different regions (the three presented in Figures 3 and 4 and two extra positions near the cod ligands). The relative position of the anion (Rh $\cdots$ B distance and Rh $\cdots$ B–F angles) was optimized, keeping fixed the geometry of the cation.

**Structural Analysis.** The structural data for the Figure 8 were retrieved with the help of the Cambridge Structural Database (Version 5.25, November 2003, first update, January 2004).<sup>42</sup> Our search included compounds  $[M(REpz_3)L_2]$  and  $[M(Epz_4)L_2]$  in which E is a main element such as C or B, and M is a  $d^8$  ion of group 9, 10, or 11.

**Acknowledgment.** Financial support of this work was provided by the Spanish DGI (Projects BQU2002-04110-C02-02, BQU2002-04033-C02-01, and BQU2003-03582) and by Generalitat de Catalunya through Grants SGR2001-0179 and SGR2001-0044. The computing resources at the Centre de Supercomputació de Catalunya (CESCA) were made available in part through a grant from Fundació Catalana per a la Recerca (FCR) and Universitat de Barcelona.

**Supporting Information Available:** Tables containing atomic coordinates of the optimized structures for minima and transition states given in Tables 2, 4, and 5. Main data for  $d^8$ - $[M(Tp^R)L_2]$  complexes from the Cambridge Structural Database. This material is available free of charge via the Internet at <http://pubs.acs.org>.

OM0497660

(42) Allen, F. H.; Kennard, O. *Chem. Des. Autom. News* **1993**, *8*, 31.